

Insights into the genomic landscape of MYD88 wild-type Waldenström macroglobulinemia

Zachary R. Hunter,^{1,2} Lian Xu,¹ Nickolas Tsakmaklis,¹ Maria G. Demos,¹ Amanda Kofides,¹ Cristina Jimenez,¹ Gloria G. Chan,¹ Jiaji Chen,¹ Xia Liu,¹ Manit Munshi,¹ Joshua Gustine,¹ Kirsten Meid,¹ Christopher J. Patterson,¹ Guang Yang,^{1,2} Toni Dubeau,¹ Mehmet K. Samur,^{2,3} Jorge J. Castillo,^{1,2} Kenneth C. Anderson,^{2,3} Nikhil C. Munshi,^{2,3} and Steven P. Treon^{1,2}

¹Bing Center for Waldenström's Macroglobulinemia, Dana-Farber Cancer Institute, Boston, MA; ²Harvard Medical School, Boston, MA; and ³Jerome Lipper Myeloma Center, Dana-Farber Cancer Institute, Boston, MA

Key Points

- Mutations affecting NF-κB, epigenomic regulation, or DNA damage repair were identified in MYD88 wild-type WM.
- NF-κB pathway mutations were downstream of BTK, and many overlapped with those found in aggressive B-cell lymphomas.

Activating *MYD88* mutations are present in 95% of Waldenström macroglobulinemia (WM) patients, and trigger NF-κB through BTK and IRAK. The BTK inhibitor ibrutinib is active in *MYD88*-mutated (*MYD88^{MUT}*) WM patients, but shows lower activity in *MYD88* wild-type (*MYD88^{WT}*) disease. *MYD88^{WT}* patients also show shorter overall survival, and increased risk of disease transformation in some series. The genomic basis for these findings remains to be clarified. We performed whole exome and transcriptome sequencing of sorted tumor samples from 18 *MYD88^{WT}* patients and compared findings with WM patients with *MYD88^{MUT}* disease. We identified somatic mutations predicted to activate NF-κB (*TBL1XR1*, *PTPN13*, *MALT1*, *BCL10*, *NFKB2*, *NFKBIB*, *NFKBIZ*, and *UDRL1F*), impart epigenomic dysregulation (*KMT2D*, *KMT2C*, and *KDM6A*), or impair DNA damage repair (*TP53*, *ATM*, and *TRRAP*). Predicted NF-κB activating mutations were downstream of BTK and IRAK, and many overlapped with somatic mutations found in diffuse large B-cell lymphoma. A distinctive transcriptional profile in *MYD88^{WT}* WM was identified, although most differentially expressed genes overlapped with *MYD88^{MUT}* WM consistent with the many clinical and morphological characteristics that are shared by these WM subgroups. Overall survival was adversely affected by mutations in DNA damage response in *MYD88^{WT}* WM patients. The findings depict genomic and transcriptional events associated with *MYD88^{WT}* WM and provide mechanistic insights for disease transformation, decreased ibrutinib activity, and novel drug approaches for this population.

Introduction

Activating *MYD88* and *CXCR4* activations are present in 95% to 97% and 35% to 40% of Waldenström macroglobulinemia (WM) patients, respectively.¹ Among WM patients who harbor an *MYD88* mutation (*MYD88^{MUT}*), nearly all carry the amino acid substitution p.Leu265Pro., making the identification of this mutation an important part of the diagnostic workup of WM.² At the protein level, *MYD88^{MUT}* triggers NF-κB pro-survival signaling through BTK and IRAK4/IRAK1, and activates the SRC family member HCK that triggers BTK, AKT, and ERK1/2 signaling.^{3,4} Ibrutinib blocks BTK and HCK activity and is highly active in *MYD88^{MUT}*, but less so in *MYD88^{WT}* WM, suggesting important differences in the molecular pro-survival signaling for these 2 WM variants.⁵⁻⁷ In some series, those with *MYD88^{WT}* disease also showed increased risk of transformation to diffuse large B-cell lymphoma (DLBCL) and/or decreased overall survival (OS).⁸⁻¹⁰ *CXCR4* mutations that impact bone marrow (BM) disease burden, immunoglobulin M (IgM) secretion, symptomatic hyperviscosity, and drug resistance are

nearly always found in those patients with *MYD88*^{MUT} WM.^{1,8,11,12} Although these findings allude to important biological differences between *MYD88*^{MUT} and *MYD88*^{WT} disease, the underlying genomic and transcriptional landscape of *MYD88*^{WT} WM remains to be clarified. We therefore performed whole exome sequencing (WES) and transcriptome sequencing of the *MYD88*^{WT} WM and compared the findings with *MYD88*^{MUT} WM.

Patients and methods

The study was approved by Dana Farber/Harvard Cancer Center institutional review board, and patients provided written consent. Lymphoplasmacytic cells were collected by CD19⁺ MACS microbead selection (Miltenyi-Biotec, Auburn, CA) from BM aspirates of 18 consecutive patients meeting clinicopathological criteria for WM and *MYD88*^{WT} disease following allele-specific polymerase chain reaction for detection of *MYD88* L265P mutations and Sanger sequencing to exclude non-L265P *MYD88* mutations.^{6,13} Baseline clinical information is shown in Table 1. For 12 patients, CD19-depleted peripheral blood mononuclear cells were available and used to prepare germline DNA as before.¹³⁻¹⁵ Fifty base-pair paired-end RNA sequencing libraries were generated using NEBNext Ultra RNA library prep kit (New England Biolabs, Ipswich, MA). WES libraries were constructed using SureSelect (Agilent, Santa Clara, CA) for 150 base pair paired-end sequencing. For tumor/germline paired samples, small variants were analyzed using both *Strelka* (<https://github.com/Illumina/strelka>) and *MuTect2* (<https://software.broadinstitute.org/gatk/>). Unpaired WM samples were analyzed by *GATK HaplotypeCaller* (<https://software.broadinstitute.org/gatk/>). Mutations in unpaired patients were assessed for genes known to be relevant to WM and/or related lymphomas. Mutations were filtered for those that affected amino acid coding and were present in a gene that had measurable gene expression in healthy donor and/or WM samples. Somatic structural variants were detected using *Manta* (<https://github.com/Illumina/manta>); copy number alterations were called using *Control-FREEC* (<http://boevalab.com/FREEC/>). Variants were annotated using the *Variant Effect Predictor* (<https://github.com/Ensembl/ensembl-vep>). RNA sequencing reads were aligned using *STAR* (<https://github.com/alexdobin/STAR>) and quantified using *Salmon* (<https://combine-lab.github.io/salmon/>). Statistical analysis was performed using R, and Bioconductor packages *limma*, *edgeR*, and *tximport* were used to calculate *voom*-based differential gene expression testing. The *DESeq2* package was used for regularized log transformation for clustering analysis and *camera* was used to calculate gene set enrichment using the publicly available MSigDB data set (<http://bioinf.wehi.edu.au/software/MSigDB/>). Sequencing data have been applied for deposition in the National Center for Biotechnology Information's Short Read Archive. Results were compared with our previous genome, transcriptome, and OS findings for *MYD88*^{MUT} WM patients.^{9,14-16} The survival from WM diagnosis, defined as the time between WM diagnosis to last follow-up or death, was estimated using the Kaplan-Meier method. All reported *P* values have been adjusted using the false discovery rate correction when appropriate.

Coded deidentified samples were collected under an approved sample collection protocol, institutional review board number 07-150.

Results

A median of >90.9 (range, 62.6-137.4) million reads were successfully mapped and paired following WES. Removing

Table 1. Patient clinical characteristics

	Median	Range or %
Age, y	59	42-81
Sex	10 males/8 females	NA
BM, %	12.5	2.5-80
slgM, mg/dL	2625	610-5620
Hb, g/dL	11.0	8.1-14.4
Adenopathy	9 (50%)	NA
Splenomegaly	7 (38.8%)	NA
Prior therapies	1	0-4
Untreated, n	8	44.4%
Previously treated, n	10	55.5%
Rituximab monotherapy	2	20.0%
Alkylators	7	70.0%
Nucleoside analogs	5	50.0%
Proteasome inhibitors	5	50.0%

Hb, hemoglobin; NA, not available; slgM, serum IgM.

multimapping and duplicate reads resulted a median coverage of 157 (range, 96-230) reads per base pair over the target regions. Aligned data files were further analyzed with ContEst (<http://www.broadinstitute.org/cancer/cga/contest>) revealing minimal sample cross contamination with median estimated contamination levels of 0.05% (range, 0.02%-0.11%). The median number of somatic mutations per patient was 33 (range, 8-294; Figure 1A). Somatic variants for *MYD88*^{WT} patients fell into 3 broad categories and included those predicted to (1) trigger NF- κ B; (2) impart epigenomic dysregulation; and (3) impair DNA damage repair (DDR). The key mutation findings and predicted protein changes are shown in Table 2. A complete list of variants is reported in supplemental Table 1. Mutations predicted to activate NF- κ B were observed in 12/18 (66.7%) patients and included *TBL1XR1*, *PTPN13*, *MALT1*, *BCL10*, *NFKB1*, *NFKB2*, *NFKBIB*, *NFKBIZ*, and *UDL1F* (Figure 1B). Although many of these variants were previously identified in patients with aggressive B-cell lymphomas, novel recurring mutations also emerged.¹⁷⁻¹⁹ *TBL1XR1* mutations that are also found in DLBCL and primary central nervous system lymphoma were identified in 5 (28%) *MYD88*^{WT} patients, and included missense, nonsense, and frameshift mutations. Two patients each harbored 2 different *TBL1XR1* mutations. *TBL1XR1* mutations occurred at sites within or proximal to WD40 domains (Figure 1C) that are known to trigger *TBL1XR1*/nuclear receptor corepressor binding and degradation of nuclear receptor corepressor leading to activation of NF- κ B and JUN pro-survival signaling.²⁰

Somatic mutations in the phosphatase *PTPN13* were observed in 4 (22%) patients, occurring within the PDZ, FERM, and KIND domains (Figure 1C). The PDZ domain binds to IKBA, an essential cytosolic gatekeeper of NF- κ B.²¹ Loss of *PTPN13* function leads to tyrosine phosphorylation of IKBA, resulting in nuclear translocation of NF- κ B. Other mutations predicted to alter NF- κ B signaling included those in the CBM complex (*MALT1*, *BCL10*) in 3 (17%), and *NFKB2* in 2 (11%) patients, and *NFKB1*, *NFKBIB*, *NFKBIZ*, and *UFD1L*, which were observed once. The 2 *MALT1* variants

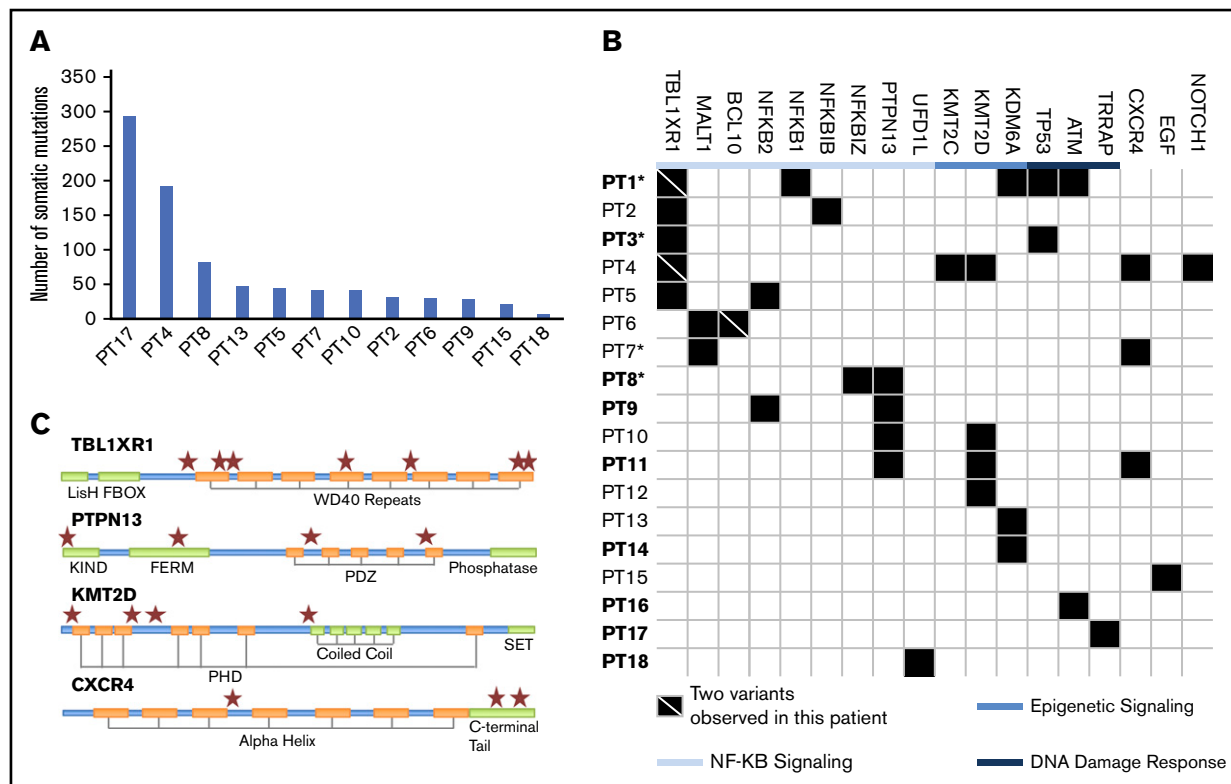


Figure 1. Mutations identified in *MYD88*^{WT} WM by whole exome sequencing. (A) The median number of somatic mutations for patients with paired tumor/germline samples was 33 and the number of mutations per patient for these individuals are shown. (B) Somatic mutations were associated with NF- κ B signaling, epigenetic regulation, and DNA damage response. Each row represents a unique patient. Patient identifiers in bold type indicate that the patient is deceased. *Patients with disease that later transformed. (C) Location of conserved motifs in the protein coding domains of top affected genes are shown. ★Location of a somatic mutation.

were nonsense mutations 23 base pairs apart and predicted for truncation of the C-terminal domain with loss of a TRAF6-binding site. Mutations at this site have not been previously reported, although functional studies suggest a critical role in preventing *MALT1* degradation and stabilizing the CBM complex.²² One patient carried both nonsense and frameshift mutations in the C-terminal domain of *BCL10*; these are similar to those in MALT and follicular lymphomas that abrogate pro-apoptotic activity and promote NF- κ B activation.²³ Structural variant analysis also revealed deletions removing the DEATH/PEST domain of *NFKB2* in 2 patients covering amino acids 691 through 822 and 711 through 839, respectively. Deletions in this region are associated with constitutive NF- κ B activation in myeloma.²⁴

Somatic mutations in the chromatin-modifying genes (CMG) *KMT2D*, *KDM6A*, and *KMT2C* were also observed in 4 (22%), 3 (17%), and 1 (6%) of the *MYD88*^{WT} WM patients, respectively. Mutations in the H3 lysine 4 methyltransferases *KMT2D* and *KMT2C* are commonly found in DLBCL and follicular non-Hodgkin lymphoma patients.^{17,18,25} Knockout studies have suggested a partial functional redundancy for these CMG.²⁵ In *KMT2D* murine knockout models, reduced class-switched B cells were observed following immunization, a finding consistent with defective B-cell maturation and/or class switching.²⁵ Mutations in the DDR genes *TP53* 2/18 (11%), *ATM* 1/18 (6%), and *TRRAP* 1/18 (6%) were also observed, and the *TRRAP*-mutated patient (patient 17) exhibited the highest number of somatic variants in this series (Figure 1A). A role for these mutations in NF- κ B-driven

lymphomagenesis is supported by previous functional studies, along with high rates of somatic mutations in *TRRAP*-mutated patients.²⁶⁻²⁸

Other mutations included *CXCR4* in 3/18 (17%) patients (Figure 1C), 2 of whom had frameshift mutations within the C-terminal domain as those found in *MYD88*^{MUT} WM patients.¹¹ A third mutation (R134S) was identified in the intracellular 2 domain; these mutations have not been previously reported in *CXCR4*-mutated WM patients. Substitutions at R134 have been demonstrated to affect inhibitory G protein alpha subunit (G_{ai}) activation.²⁹ In addition, 1 *NOTCH1* and 1 *EGF* mutation were observed. Analysis of copy number alterations revealed no recurring events, but was remarkable for the absence of chromosome 6q deletions that are present in half of *MYD88*-mutated WM patients, and target genes regulating BTK, BCL2, NF- κ B, and apoptosis signaling.³⁰ To better understand the relevance of these mutations in relationship to *MYD88* mutation status, we compared the WES findings from this study with those from our previous whole genome sequencing of 53 *MYD88*^{MUT} WM patients.^{14,15} Although many of the mutated genes in *MYD88*^{WT} patients were also found in *MYD88*^{MUT} patients, *TBL1XR1* and *MALT1* mutations were observed in *MYD88*^{WT} patients only ($P = .001$ and 0.062 , respectively), whereas those with *KDM6A* ($P = .052$) and *KMT2D* ($P = .065$) showed a trend toward enrichment in *MYD88*^{WT} patients (Figure 2A).

With a median follow-up of 72.1 months (range, 13.2-176.9) from diagnosis, 4 (22.2%) patients transformed to DLBCL. Nine (50%)

Table 2. Observed somatic mutations in MYD88WT WM

Gene	Consequence	Chr	Position	Variant	Protein	COSMIC	CADD
<i>BCL10</i>	Nonsense	1	85733609	T/A	p.L135R>*	COSM220638	38
<i>BCL10</i>	Frameshift	1	85733357-8	-/AGAGTTTGACACAAG	p.-/218-219LVQTX		NA
<i>CXCR4</i>	Deletion	2	136872441-82	TCTGTTCCACTGAGTC TGAGTCTCAAGTTTT CACTCCAGCTaa/taa	p.SVSTESSESSFH SS*339-353*		NA
<i>CXCR4</i>	Frameshift	2	136872566-7	-/T	p.T315NX		NA
<i>CXCR4</i>	Missense	2	136873098	G/T	p.R134S		26.9
<i>NFKB1Z</i>	Missense	3	101574709	A/C	p.K45T		26.3
<i>TBL1XR1</i>	Missense	3	176743302	A/G	p.S10L>S		26.1
<i>TBL1XR1</i>	Missense	3	176744171	G/A	p.S503L	COSM5000343	34
<i>TBL1XR1</i>	Splice acceptor	3	176750925	C/G	NA		25.8
<i>TBL1XR1</i>	Deletion	3	176756175-7	AAG/-	p.SC924-325C	COSM3205534	NA
<i>TBL1XR1</i>	Nonsense	3	176767829	G/A	p.Q220*		39
<i>TBL1XR1</i>	Missense	3	176768267	C/G	p.G187GR		33
<i>TBL1XR1</i>	Frameshift	3	176769342	T/-	p.N126NX	COSM1420706	34
<i>PTPN13</i>	Missense	4	87556423	T/A	p.L5Q		33
<i>PTPN13</i>	Missense	4	87656789	G/T	p.A732S	COSM5019859	27.6
<i>PTPN13</i>	Missense	4	87683919	A/C	p.N1198T		3.849
<i>PTPN13</i>	Missense	4	87696460	C/A	p.P1882Q	COSM481650	25.4
<i>NFKB1</i>	Missense	4	103459060	G/A	p.G69R		31
<i>KMT2C</i>	Nonsense	7	151891205	C/A	p.G1517*	COSM3304224	41
<i>NOTCH1</i>	Nonsense	9	139390945	G/A	p.Q2416*	COSM4775108	41
<i>NFKB2</i>	Deletion	10	104160996-1855	NA	NA		NA
<i>NFKB2</i>	Deletion	10	104160849-1688	NA	NA		NA
<i>ATM</i>	Nonsense	11	108175504	C/T	p.Q1867*		37
<i>ATM</i>	Missense	11	108204685	T/C	p.M2667T		26.3
<i>KMT2D</i>	Frameshift	12	49433373-4	-/G CCG CCCCCCT	p.-/2891-2692AAPX		NA
<i>KMT2D</i>	Missense	12	49445543	T/G	p.E641D		5.499
<i>KMT2D</i>	Missense	12	49446710	G/T	p.P367Q		11.92
<i>KMT2D</i>	Frameshift	12	49448408	G/-	p.G101X'		NA
<i>TP53</i>	Missense	17	7577108	C/A	p.C277F	COSM562338	34
<i>TP53</i>	Missense	17	7577114	C/A	p.C275F	COSM99932	34
<i>MALT1</i>	Nonsense	18	56414859	C/T	p.Q743*		36
<i>MALT1</i>	Nonsense	18	56414882	C/A	p.Y750*		36
<i>NFKB1B</i>	Frameshift	19	39398226-7	CT/-	p.P299X	COSM5081722	NA
<i>UFD1L</i>	Missense	22	19443248	C/A	p.G145V		23.6

CADD, combined annotation dependent depletion; chr, chromosome; COSMIC, Catalogue of Somatic Mutations in Cancer.

Table 2. (continued)

Gene	Consequence	Chr	Position	Variant	Protein	COSMIC	CADD
KDM6A	Missense	X	44911044	T/A	p.L249I		25.4
KDM6A	Frameshift	X	44942757	G/-	p.V1113X	COSM5031082	NA
KDM6A	Frameshift	X	44922936-7	-/GGAAGTGGAAAGT AAT GGAAC GTGCC	p./599- 600GSGSNGNVX		NA

CADD, combined annotation dependent depletion; chr, chromosome; COSMIC, Catalogue of Somatic Mutations in Cancer.

died, including 3 from disease transformation. The genomic mutations found in transformed patients included *TBL1XR1*, *TP53*, *NFKB1*, *NFKB2*, and *MALT1* somatic mutations, all of which have been identified in DLBCL patients.^{17,18} *MYD88*^{WT} patients had a significantly lower median OS relative to patients with *MYD88*^{MUT} disease. The estimated median OS for the 18 *MYD88*^{WT} patients was 167 months; a median follow-up of 73.8 months was insufficient to calculate the predicted median for the cohort of 262 *MYD88*^{MUT} patients diagnosed over the same period (log-rank $P < .0001$). Genomic findings were aggregated into NF- κ B signaling, epigenetic signaling, and DDR categories and evaluated for their effect on OS. Particularly striking was the exceedingly poor survival in patients with DDR mutations, in whom the median OS was 29.9 months (range, 13.2-33.1), as shown in Figure 2B. No significant differences in OS were observed when stratifying the *MYD88*^{WT} population by the other 2 categories. Constructing a Cox proportional hazard model accounting for sex, age at diagnosis, *MYD88* mutation status, and the presence of DDR mutations revealed hazard ratios of 8.5 and 77.9 for *MYD88*^{WT}*DDR*^{WT} and *MYD88*^{WT}*DDR*^{MUT}, respectively, relative to *MYD88*^{MUT} WM patients ($P < .001$ for both comparisons).

Analysis of the *MYD88*^{WT} WM transcriptome revealed a distinct transcriptional profile (Figure 3A). However, principal component analysis of the top 500 high-variance genes revealed a clustering of *MYD88*^{WT} and *MYD88*^{MUT} WM samples, regardless of *CXCR4* mutation status that was distinct from healthy donor peripheral blood B, memory B, and plasma cells (Figure 3B). These findings were recapitulated in the supervised clustering of the top 100 most statistically significant differentially expressed genes between healthy donor memory B cells and *MYD88*^{WT} WM samples, in which gene expression levels were very similar between all WM samples regardless of *MYD88* and *CXCR4* mutation status (Figure 3C). Likewise, the contrast between healthy donor memory B cells and *MYD88*^{WT} samples found significant log₂ fold change (LFC) overexpression of genes we had previously associated with WM, including *DNTT* (LFC, 12.4; $P = .005$), *RAG1* (LFC, 8.1; $P = .008$), *RAG2* (LFC, 10.0; $P < .001$), *CXCL12* (LFC, 11.8; $P = .002$), *VCAM1* (LFC, 10.6; $P = .001$), *IGF1* (LFC, 7.0; $P < .001$), *BMP3* (LFC, 7.0; $P = .005$), *CD5L* (LFC, 10.0; $P = .002$), and *B2M* (LFC, 1.1; $P = .022$).¹⁵ These findings are likely to explain many of the shared clinical and morphological characteristics among WM patients, regardless of their underlying *MYD88* mutation status. The exceptions were *CXCR4*, *BCL2*, and *BAX*, which were not significantly different from healthy donor controls in *MYD88*^{WT} samples.

Comparisons of gene expression based on *MYD88* mutation status revealed 291 significantly dysregulated genes that can be seen in supplemental Table 2. Many of the genes we previously associated with *MYD88*^{WT} WM were validated in this larger cohort including *IL6* (LFC, -3.7; $P = .022$), *TNFAIP3* (LFC, -1.5; $P = .04$), *NFKBIZ* (LFC, -1.8; $P = .034$), *PIM1* (LFC, -2.1; $P < .001$), *PIM2* (LFC, -1.4; $P = .038$), *CD40* (LFC, -1.4; $P = .037$), and *CD86* (LFC, 2.7; $P = .024$). A significant dysregulation in a number of highly relevant novel genes including *RASSF6* (LFC, -6.1; $P = .02$), *EIF5A2* (LFC, 2.4; $P = .008$), *CCL22* (LFC, -4.5; $P = .034$), *CCR7* (LFC, -2.7; $P = .006$), *LTK* (LFC, 2.0; $P = .028$), *VEGFA* (LFC, -2.7; $P = .027$), *PRDM8* (LFC, -2.6; $P < .001$), *PRDM1* (LFC, -3.0; $P = .001$), and *XBP1*

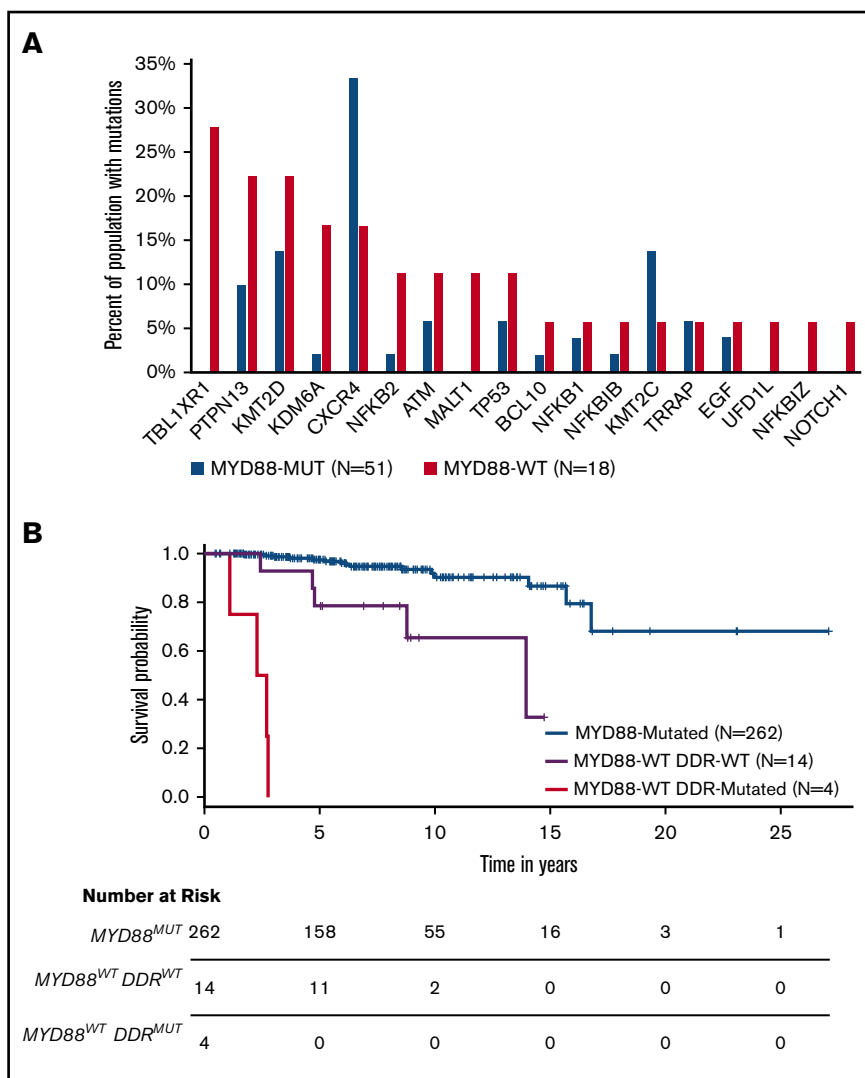


Figure 2. Comparison of findings for *MYD88^{WT}* and *MYD88^{MUT}* WM. Comparison of somatic mutation frequencies between *MYD88^{WT}* and *MYD88^{MUT}* WM patients. (A) Data for mutation frequencies for 53 *MYD88^{MUT}* WM patients were acquired from our previous whole genome sequencing results, using high-quality somatic variants supported by at least 3 reads.^{10,11} (B) Kaplan-Meier curves for overall survival from time of diagnosis for WM patients with *MYD88^{MUT}*, and *MYD88^{WT}* with and without DDR mutations (log-rank $P < .0001$).

(LFC, -1.9 ; $P = .028$) was also found in this expanded cohort. Gene set enrichment analysis identified significant enrichment for the upregulation of E2F, MYC, PIK3-AKT-MTOR, and G2M checkpoint signaling targets ($P \leq .009$ for all) as well as the downregulation of inflammatory response genes ($P = .023$) and TNFA signaling through NF- κ B ($P < .001$).

Discussion

This is the first study to focus on the genome and transcriptome of *MYD88^{WT}* WM, an infrequent subtype of WM that is remarkable in certain studies for an increased risk of disease transformation, lower response to ibrutinib, and shortened OS.^{5-10,31} Distinct patterns of mutations were identified among *MYD88^{WT}* patients, including those affecting NF- κ B signaling, epigenomic regulators, and those in DDR genes, and were independent of prior treatment status. The most common mutations involved those affecting genes in NF- κ B signaling that were identified in 12/18 (66.7%) *MYD88^{WT}* patients, and included *TBL1XR1*, *NFKBIB*, *NFKBIZ*, *NFKB2*, *MALT1*, *BCL10*, and *UDRLIF*. Although mutations in these genes are rare or absent in *MYD88^{MUT}* WM disease, they are found in aggressive lymphomas.¹⁷⁻¹⁹ *TBL1XR1* mutations that were identified in 5

patients, including 2 patients who each had 2 mutations that are of particular interest given their frequent presence in activated B cell-like DLBCL and primary central nervous system lymphoma.¹³⁻¹⁵ These diseases are also recognized for their high frequency of recurring *MYD88* mutations that are exclusive of *TBL1XR1* mutations, suggesting that the actions of the latter may mimic at least in part those of activating *MYD88* mutations.¹³⁻¹⁵ In addition to mutations in *TBL1XR1*, many of the other NF- κ B pathway mutations identified in this study are found in aggressive B-cell lymphomas. Taken together, these findings may provide a genomic explanation for the increased risk of disease transformation^{9,10} and accompanying shorter survival observed in our previous study for *MYD88^{WT}* WM patients.⁹ Somatic mutations in CMG were also observed in 8 (44.4%) *MYD88^{WT}* patients. *KMT2D* mutations were the most common CMG mutations observed in *MYD88^{WT}* WM patients, and are present in 30% of DLBCL patients. Varettoni et al³² recently reported *KMT2D* mutations in 24% of *MYD88^{MUT}* WM patients, although these were primarily subclonal and their clinical course relative to patients without *KMT2D* mutations was not clarified. The mechanistic pathways by which CMG mutations promote WM pro-survival

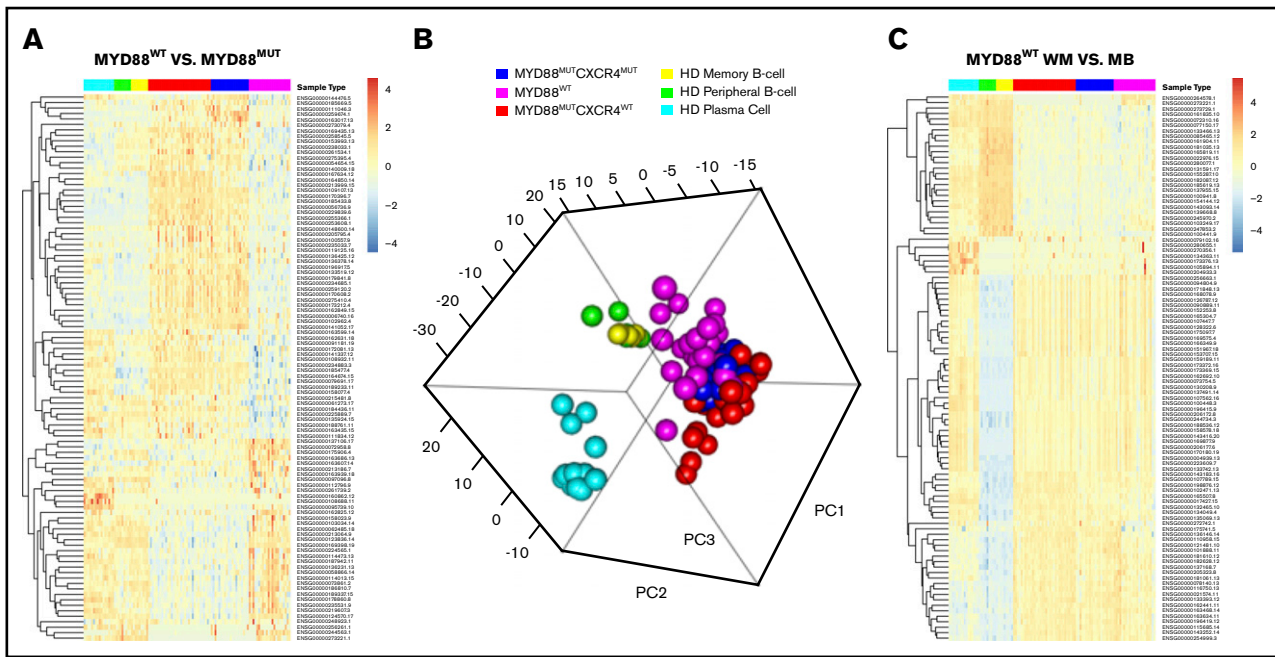


Figure 3. Findings from next-generation gene expression studies in *MYD88*^{WT} WM. (A) The top 100 most statistically significant genes between samples from 18 *MYD88*^{WT} and 75 *MYD88*^{MUT} patients are shown, demonstrating a uniform gene signature associated with the *MYD88*^{WT} population. (B) Principal component analysis of the top 500 high variance genes revealed a clustering of *MYD88*^{WT} and *MYD88*^{MUT} WM samples, regardless of *CXCR4* mutation status that was distinct from healthy donor peripheral B, memory B, and plasma cells. (C) These findings were also recapitulated in the supervised clustering of the top 100 most statistically significant differentially expressed genes between healthy donor memory B cells and *MYD88*^{WT} WM samples, in which gene expression levels were very similar between all WM samples regardless of *MYD88* and *CXCR4* mutation status.

signaling deserves further study given their frequent occurrence in WM.

Particularly concerning were *MYD88*^{WT} patients who presented with DDR mutations. Compared with patients with *MYD88*^{MUT} and *MYD88*^{WT} disease lacking DDR mutations, those with *MYD88*^{WT} disease with DDR mutations represented a subset with ultra-high-risk disease. A similar observation has also been made in myeloma patients.³³ Although *TP53* mutations are uncommon in WM, they are present in *MYD88*-mutated patients.^{32,34,35} Their association with poor outcome in *MYD88*-mutated patients has previously been reported.^{34,35} Last, *CXCR4* activating mutations found in 30% to 40% of *MYD88*^{MUT} patients were identified in *MYD88*^{WT} patients, although the frequency of these mutations was lower. Only 2 (9%) of the *MYD88*^{WT} patients had C-terminal variants that promote WHIM-like signaling, as found in *MYD88*^{MUT} WM patients. The significance of a third *CXCR4* variant (R134S) identified in 1 patient remains unclear. All 3 of these *CXCR4*-mutated patients also had mutations affecting NF-κB signaling, akin to *MYD88*-mutated WM patients, and may therefore be amenable to therapeutics targeting *CXCR4*, such as ulocuplumab, which is being investigated in WM patients harboring both *MYD88* and *CXCR4* mutations in combination with ibrutinib (NCT03225716).

The findings of this study may also provide important insights into why WM patients with *MYD88*^{WT} disease are less responsive to ibrutinib monotherapy.⁵⁻⁷ The NF-κB pathway mutations observed in two-thirds of *MYD88*^{WT} patients were all downstream of BTK (Figure 4). NF-κB pathway inhibitors that are downstream of BTK, including proteasome inhibitors that target IKBA, and novel agents that target IKK and MALT1 may be more appropriate for these individuals.^{36,37} A mechanistic rationale for how ibrutinib fits into the

treatment of CMG and DDR-mutated *MYD88*^{WT} WM remains elusive, as does a targeted treatment approach for such patients.

An unexpected finding was the transcriptional similarity for *MYD88*^{WT} and *MYD88*^{MUT} disease relative to healthy donor B cells. This finding may well account for the many overlapping disease characteristics observed between *MYD88*^{WT} and *MYD88*^{MUT} patients.^{8,9} The transcriptional similarity between these subsets of WM may reflect the common activation of NF-κB triggered by activating mutations such as *TBL1XR1* in *MYD88*^{WT} patients and mutated *MYD88*. However, the extent of NF-κB activation may differ, because some NF-κB-regulated genes such as *IL6*, *IRAK2*, *TNFAIP3*, *NFKBIZ*, *NFKB2*, *TIRAP*, *PIM1*, and *PIM2* show lower expression in *MYD88*^{WT} vs *MYD88*^{MUT} patients. Because *MYD88* is a key mediator of innate immune signaling, additional branch points for downstream signaling exist, even in the context of NF-κB that includes AKT and ERK (via cytokines) pathways triggered by *MYD88* activation of HCK and/or BCR/SYK in WM cells.^{4,38} The existence of a “My-T-BCR supercomplex” that encompasses mutated *MYD88* and BCR components that contribute to broader signaling that includes mTOR is also supported by recent studies in activated B cell-like DLBCL.³⁹ Consistent with this notion, we observed a gene set enrichment for PI3K-AKT-MTOR signaling was observed in *MYD88*^{WT} patients; therefore, a targeted approach for treating *MYD88*^{WT} patients may entail the use of PI3K or mTOR inhibitors. In contrast to *MYD88*^{MUT} patients, those with *MYD88*^{WT} had lower levels of *BCL2* expression that were on par with the expression found in healthy donor B cells. The *BCL2* antagonist venetoclax has shown remarkable activity in WM, although *MYD88* mutation status and relative dependence on *BCL2* expression remain to be clarified.⁴⁰

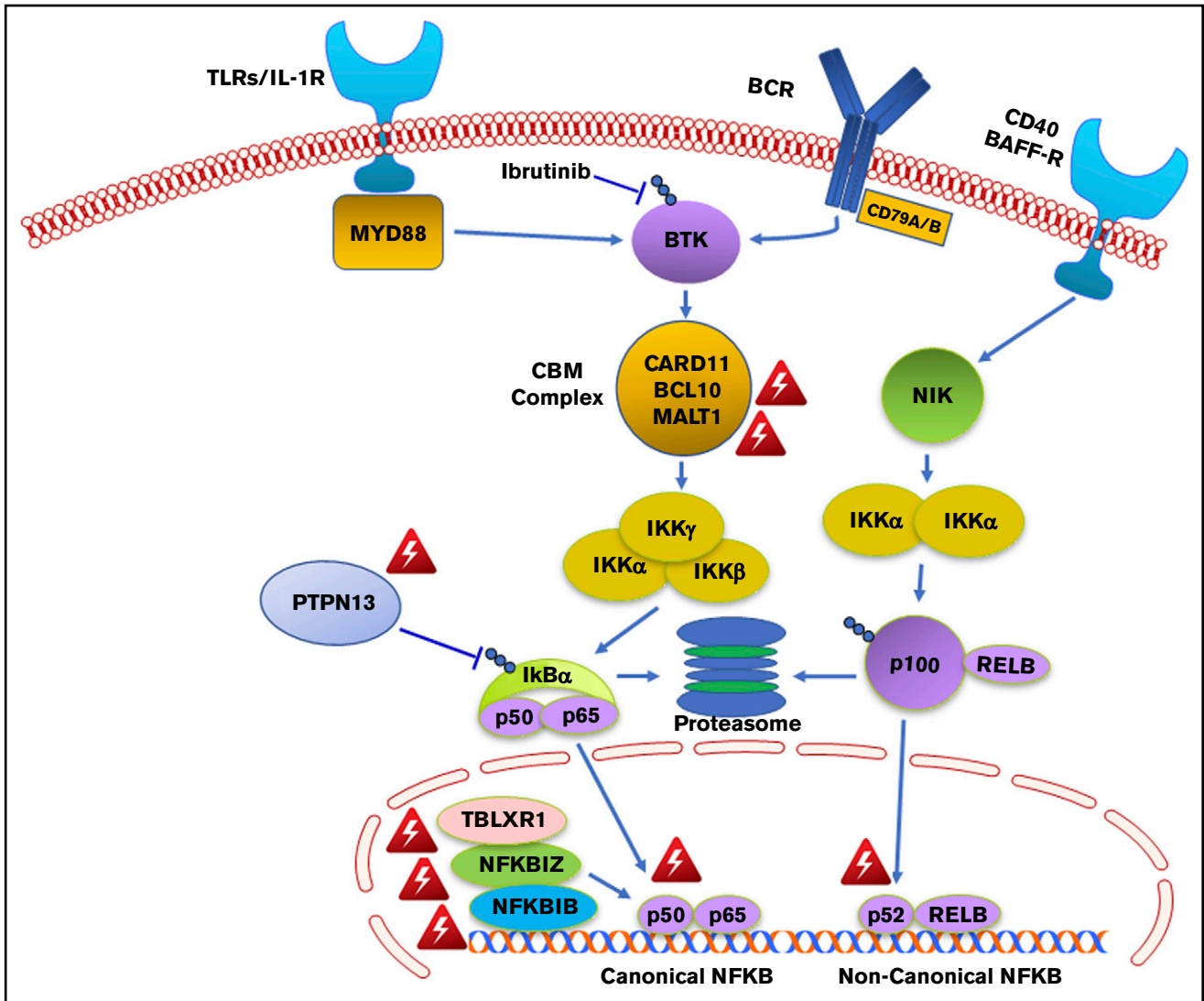


Figure 4. Genomic variants identified in MYD88 wild-type WM that affect NF- κ B signaling. Red triangle denotes variants identified by whole exome sequencing in MYD88 wild-type WM patients.

In summary, the findings depict genomic and transcriptional events associated with MYD88^{WT} WM and provide mechanistic insights for disease transformation, decreased ibrutinib activity, and novel drug approaches for this population.

Acknowledgments

The authors acknowledge the contributions of Yaoyu Wang and John Quackenbush at the Center for Cancer Computational Biology at the Dana-Farber Cancer Institute for generating the next-generation sequencing data, as well as Mathew Temple and Leutz Buon of the Dana-Farber Research Computing Center for their assistance.

The work was supported by the Orszag Family Fund for WM Research, Peter S. Bing, International Waldenström's Macroglobulinemia Foundation, Kerry Robertson Fund for WM, Leukemia and Lymphoma Society, National Institutes of Health, National Cancer Institute Development Award (grant Spore 5P50CA100707-12) (Z.R.H.), and an American Society of Hematology Scholar Award (Z.R.H.).

Authorship

Contribution: Z.R.H. and S.P.T. designed the study and wrote the manuscript; Z.R.H., M.K.S., and G.G.C. conducted the bioinformatic analysis; L.X., N.T., M.G.D., A.K., J.C., X.L., M.M., and G.Y., performed tumor cell isolation, and/or allele-specific polymerase chain reaction genotyping assays and Sanger sequencing; and S.P.T., J.J.C., C.J., K.C.A., N.C.M., C.J.P., K.M., J.G., and T.D. provided patient care, obtained samples, clinical data and/or analyzed clinical data.

Conflict-of-interest disclosure: Z.R.H., S.P.T., N.C.M., K.C.A., and J.J.C. have received consulting fees, and/or research funding from Pharmacyclics Inc., Janssen Inc., AbbVie Inc., and/or Bristol Myers Squibb. The remaining authors declare no competing financial interests.

ORCID profiles: Z.R.H., 0000-0002-1689-1691; J.J.C., 0000-0001-9490-7532; S.P.T., 0000-0001-6393-6154.

Correspondence: Steven P. Treon, Bing Center for Waldenström's Macroglobulinemia, Dana-Farber Cancer Institute, M547, 450 Brookline Ave, Boston MA 02215; e-mail: steven_treon@dfci.harvard.edu.

References

1. Hunter ZR, Yang G, Xu L, Liu X, Castillo JJ, Treon SP. Genomics, signaling, and treatment of Waldenström macroglobulinemia. *J Clin Oncol*. 2017;35(9):994-1001.
2. Castillo JJ, Garcia-Sanz R, Hatjiharissi E, et al. Recommendations for the diagnosis and initial evaluation of patients with Waldenström macroglobulinaemia: a Task Force from the 8th International Workshop on Waldenström Macroglobulinaemia. *Br J Haematol*. 2016;175(1):77-86.
3. Yang G, Zhou Y, Liu X, et al. A mutation in MYD88 (L265P) supports the survival of lymphoplasmacytic cells by activation of Bruton tyrosine kinase in Waldenström macroglobulinemia. *Blood*. 2013;122(7):1222-1232.
4. Yang G, Buhrlage SJ, Tan L, et al. HCK is a survival determinant transactivated by mutated MYD88, and a direct target of ibrutinib. *Blood*. 2016;127(25):3237-3252.
5. Treon SP, Tripsas CK, Meid K, et al. Ibrutinib in previously treated Waldenström's macroglobulinemia. *N Engl J Med*. 2015;372(15):1430-1440.
6. Treon SP, Xu L, Hunter Z. MYD88 mutations and response to ibrutinib in Waldenström's macroglobulinemia. *N Engl J Med*. 2015;373(6):584-586.
7. Dimopoulos MA, Trotman J, Tedeschi A, et al; iNNOVATE Study Group and the European Consortium for Waldenström's Macroglobulinemia. Ibrutinib for patients with rituximab-refractory Waldenström's macroglobulinaemia (iNNOVATE): an open-label substudy of an international, multicentre, phase 3 trial. *Lancet Oncol*. 2017;18(2):241-250.
8. Treon SP, Cao Y, Xu L, Yang G, Liu X, Hunter ZR. Somatic mutations in MYD88 and CXCR4 are determinants of clinical presentation and overall survival in Waldenström macroglobulinemia. *Blood*. 2014;123(18):2791-2796.
9. Treon SP, Gustine J, Xu L, et al. MYD88 wild-type Waldenström macroglobulinaemia: differential diagnosis, risk of histological transformation, and overall survival. *Br J Haematol*. 2018;180(3):374-380.
10. Abeykoon JP, Paludo J, King RL, et al. MYD88 mutation status does not impact overall survival in Waldenström macroglobulinemia. *Am J Hematol*. 2018;93(2):187-194.
11. Poulain S, Roumier C, Venet-Cailault A, et al. Genomic landscape of CXCR4 mutations in Waldenström macroglobulinemia. *Clin Cancer Res*. 2016;22(6):1480-1488.
12. Xu L, Hunter ZR, Tsakmaklis N, et al. Clonal architecture of CXCR4 WHIM-like mutations in Waldenström macroglobulinaemia. *Br J Haematol*. 2016;172(5):735-744.
13. Xu L, Hunter ZR, Yang G, et al. MYD88 L265P in Waldenström macroglobulinemia, immunoglobulin M monoclonal gammopathy, and other B-cell lymphoproliferative disorders using conventional and quantitative allele-specific polymerase chain reaction [published correction appears in *Blood*. 2013;121(26):5259]. *Blood*. 2013;121(11):2051-2058.
14. Treon SP, Xu L, Yang G, et al. MYD88 L265P somatic mutation in Waldenström's macroglobulinemia. *N Engl J Med*. 2012;367(9):826-833.
15. Hunter ZR, Xu L, Yang G, et al. The genomic landscape of Waldenström macroglobulinemia is characterized by highly recurring MYD88 and WHIM-like CXCR4 mutations, and small somatic deletions associated with B-cell lymphomagenesis. *Blood*. 2014;123(11):1637-1646.
16. Hunter ZR, Xu L, Yang G, et al. Transcriptome sequencing reveals a profile that corresponds to genomic variants in Waldenström macroglobulinemia. *Blood*. 2016;128(6):827-838.
17. Schmitz R, Wright GW, Huang DW, et al. Genetics and pathogenesis of diffuse large B-cell lymphoma. *N Engl J Med*. 2018;378(15):1396-1407.
18. Chapuy B, Stewart C, Dunford AJ, et al. Molecular subtypes of diffuse large B cell lymphoma are associated with distinct pathogenic mechanisms and outcomes [published correction appears in *Nat Med*. 2018;24:1290-1292]. *Nat Med*. 2018;24(5):679-690.
19. Gonzalez-Aguilar A, Idbaih A, Boisselier B, et al. Recurrent mutations of MYD88 and TBL1XR1 in primary central nervous system lymphomas. *Clin Cancer Res*. 2012;18(19):5203-5211.
20. Jung H, Yoo HY, Lee SH, et al. The mutational landscape of ocular marginal zone lymphoma identifies frequent alterations in TNFAIP3 followed by mutations in TBL1XR1 and CREBBP. *Oncotarget*. 2017;8(10):17038-17049.
21. Maekawa K, Imagawa N, Naito A, Harada S, Yoshie O, Takagi S. Association of protein-tyrosine phosphatase PTP-BAS with the transcription-factor-inhibitory protein I κ B α through interaction between the PDZ1 domain and ankyrin repeats. *Biochem J*. 1999;337(Pt 2):179-184.
22. Ginster S, Bardet M, Unterreiner A, et al. Two Antagonistic MALT1 auto-cleavage mechanisms reveal a role for TRAF6 to unleash MALT1 activation. *PLoS One*. 2017;12(1):e0169026.
23. Du MQ, Peng H, Liu H, et al. BCL10 gene mutation in lymphoma. *Blood*. 2000;95(12):3885-3890.
24. Annunziata CM, Davis RE, Demchenko Y, et al. Frequent engagement of the classical and alternative NF- κ B pathways by diverse genetic abnormalities in multiple myeloma. *Cancer Cell*. 2007;12(2):115-130.
25. Green MR. Chromatin modifying gene mutations in follicular lymphoma. *Blood*. 2018;131(6):595-604.
26. Gostissa M, Bianco JM, Malkin DJ, et al. Conditional inactivation of p53 in mature B cells promotes generation of nongerminal center-derived B-cell lymphomas. *Proc Natl Acad Sci USA*. 2013;110(8):2934-2939.
27. Hathcock KS, Padilla-Nash HM, Camps J, et al. ATM deficiency promotes development of murine B-cell lymphomas that resemble diffuse large B-cell lymphoma in humans. *Blood*. 2015;126(20):2291-2301.
28. Parry M, Rose-Zerilli MJ, Gibson J, et al. Whole exome sequencing identifies novel recurrently mutated genes in patients with splenic marginal zone lymphoma. *PLoS One*. 2013;8(12):e83244.

29. Berchiche YA, Chow KY, Lagane B, et al. Direct assessment of CXCR4 mutant conformations reveals complex link between receptor structure and G(α)i activation. *J Biol Chem*. 2007;282(8):5111-5115.
30. Guerrero ML, Tsakmaklis N, Xu L, et al. MYD88 mutated and wild-type Waldenström's macroglobulinemia: characterization of chromosome 6q gene losses and their mutual exclusivity with mutations in CXCR4. *Haematologica*. 2018;103(9):e408-e411.
31. Treon SP, Gustine J, Meid K, et al. Ibrutinib monotherapy in symptomatic, treatment-naïve patients with Waldenström macroglobulinemia. *J Clin Oncol*. 2018;36(27):2755-2761.
32. Varettoni M, Zibellini S, Defrancesco I, et al. Pattern of somatic mutations in patients with Waldenström macroglobulinemia or IgM monoclonal gammopathy of undetermined significance. *Haematologica*. 2017;102(12):2077-2085.
33. Walker BA, Boyle EM, Wardell CP, et al. Mutational spectrum, copy number changes, and outcome: Results of a sequencing study of patients with newly diagnosed myeloma. *J Clin Oncol*. 2015;33(33):3911-3920.
34. Poulain S, Roumier C, Bertrand E, et al. TP53 Mutation and its prognostic significance in Waldenström's macroglobulinemia. *Clin Cancer Res*. 2017;23(20):6325-6335.
35. Gustine JN, Tsakmaklis N, Demos MG, et al. TP53 mutations are associated with mutated MYD88 and CXCR4, and confer an adverse outcome in Waldenström macroglobulinaemia [published online ahead of print 5 September 2018]. *Br J Haematol*. doi:10.1111/bjh.15560.
36. Lee DF, Hung MC. Advances in targeting IKK and IKK-related kinases for cancer therapy. *Clin Cancer Res*. 2008;14(18):5656-5662.
37. Fontan L, Yang C, Kabaleeswaran V, et al. MALT1 small molecule inhibitors specifically suppress ABC-DLBCL in vitro and in vivo. *Cancer Cell*. 2012;22(6):812-824.
38. Munshi M, Liu X, Chen J, et al. Mutated MYD88 activates the BCR component SYK and provides a rationale therapeutic target in Waldenström's macroglobulinemia [abstract]. *Blood*. 2017;128(22):2984. Abstract 2539.
39. Phelan JD, Young RM, Webster DE, et al. A multiprotein supercomplex controlling oncogenic signalling in lymphoma. *Nature*. 2018;560(7718):387-391.
40. Castillo JJ, Gustine J, Meid K, et al. Prospective phase II study of venetoclax (VEN) in patients (PTS) with previously treated Waldenström macroglobulinemia (WM). Paper presented at Proceedings of the European Hematology Association. 16 June 2018. Stockholm, Sweden. Abstract S854.